AIAA 81-4104

Role of Laminar Separation Bubbles in Airfoil Leading-Edge Stalls

B. van den Berg*
National Aerospace Laboratory NLR, Amsterdam, The Netherlands

It is argued that there are two possible mechanisms for leading-edge stalls: 1) burst of the laminar separation bubble near the airfoil leading edge, and 2) turbulent boundary-layer separation in the leading-edge region. To investigate the relative importance of both mechanisms for leading-edge stalls, a theoretical analysis is made of the flow around airfoil noses. The analysis suggests that turbulent boundary-layer separation in the nose region may well be the dominant cause of leading-edge stalls, especially at higher Reynolds numbers. This conclusion is confirmed by an analysis of measured wall shear-stress data in the nose region of two modern airfoil sections. By using a suitable parameter for indicating proximity of separation, the likelihood of turbulent boundary-layer separation in the nose region is demonstrated for these two airfoil sections.

Nomenclature

a^+ = separation parameter, see Eq. (9)
c = airfoil chord
C_f = $\tau_W / \frac{1}{2}\rho U^2$, wall shear-stress coefficient
C_p = $(p-p_\infty)/\frac{1}{2}\rho U_\infty^2$, wall static-pressure coefficient
p = wall static pressure
Re_c = $U_\infty c/\nu$, airfoil Reynolds number
Re_θ = $U\theta/\nu$, boundary-layer momentum thickness Reynolds number
s = coordinate along airfoil contour
U = inviscid flow velocity
x,y = airfoil coordinates
y_n = airfoil upper surface coordinate at $x/c=0.0125$ ($x=0$ at leading edge)
α = angle of attack
ϵ = airfoil thickness parameter
θ = boundary-layer momentum thickness
λ = $\frac{\theta^2}{\nu}\frac{dU}{ds}$, pressure gradient parameter
Λ = $\frac{\theta_s^2}{\nu}\frac{\Delta U}{\Delta s}$, Gaster's bubble parameter
ν = kinematic viscosity
ρ = density
τ_W = wall shear stress
ψ = parameter related to surface coordinate s, see Eq. (3)

Subscripts

s = value at laminar separation point
∞ = freestream value
0 = value at stagnation point

Introduction

At least three types of stall may be distinguished for two-dimensional airfoils (see, e.g., Ref. 1). The type of stall considered here is the leading-edge stall. A leading-edge stall is characterized by a sudden loss of lift at the stalling angle of attack. This sudden loss of lift is generally attributed to a so-called burst of the laminar separation bubble present on the airfoil nose. Bubble burst actually means that the separated shear layer downstream of the laminar separation point fails to reattach as a turbulent boundary layer closely behind the separation point. When the small laminar separation bubble on the airfoil nose has burst, an abrupt change will occur to a flow with a large separation region and a less-loaded nose. The abrupt change of flow pattern is associated with a sudden loss of lift.

As a criterion for bubble burst the boundary-layer Reynolds number at separation was suggested by Owen and Klanfer.[2] Subsequently, Crabtree[3] proposed a criterion based on the pressure rise over the bubble. On the basis of extensive investigations on laminar separation bubbles Gaster[4] concluded that bubble burst depends on both the Reynolds number and the pressure rise over the bubble. He employed the parameters $Re_{\theta s} = U_s\theta_s/\nu$ and $\Lambda = (\theta_s^2/\nu)(\Delta U/\Delta s)$, where $\Delta U/\Delta s$ is the mean velocity gradient over the bubble length Δs. Later, calculation methods for laminar separation bubbles were developed,[5-8] that predict bubble burst in accordance with the trends indicated by Gaster.

There have been a number of investigators,[9-11] who suggested that leading-edge stalls may also be due to turbulent boundary-layer separation downstream of the bubble. They supposed that separation occurs a short distance downstream of the bubble and assumed the phenomenon to be closely associated with the bubble. More generally, however, it can be stated that when boundary-layer separation does not occur first at the airfoil trailing edge, but somewhere in the leading-edge region, the stall development will resemble that for a leading-edge bubble burst; an abrupt change of flow pattern around the airfoil will occur, which will be associated with a sudden loss of lift. This means that it is not possible to conclude from the stall development whether the stall is due to bubble burst or to turbulent boundary-layer separation in the leading-edge region.

Hence, there are two possible mechanisms for leading edge stalls: 1) burst of the laminar separation bubble near the airfoil leading edge and 2) turbulent boundary-layer separation in the leading-edge region. In the present paper it is argued that in the Reynolds number range where leading-edge stalls occur the second mechanism often will be the cause of the stall. The evidence is reached by a theoretical analysis of the flow in the leading-edge region, given in the next section. The subsequent section deals with some measurements that will show that at larger angles of attack turbulent boundary-layer separation in the leading-edge region is imminent for the two airfoil sections considered.

Analysis of the Flow near Airfoil Leading Edges

Symmetrical Joukowski airfoils are considered whose shape is given by[12]

$$y/c = 2\epsilon\{1-(x/c)\}\{(x/c)+(x/c)^2\}^{\frac{1}{2}} \quad (1)$$

where ϵ is the thickness parameter; and airfoil maximum thickness $t/c = 1.3\epsilon$. The variation of the inviscid flow velocity in the leading-edge region of such an airfoil may be written

Received April 21, 1980; revision received Nov. 4, 1980.

*Senior Research Scientist.

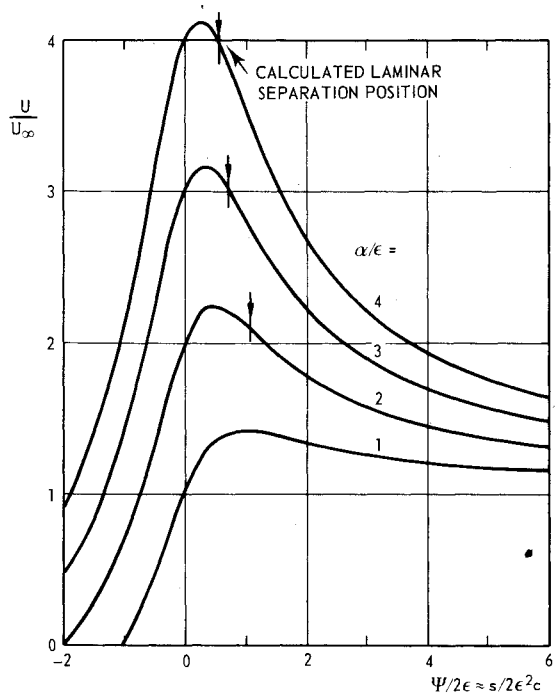

Fig. 1 Typical velocity distributions in the leading-edge region of an airfoil according to Eq. (2).

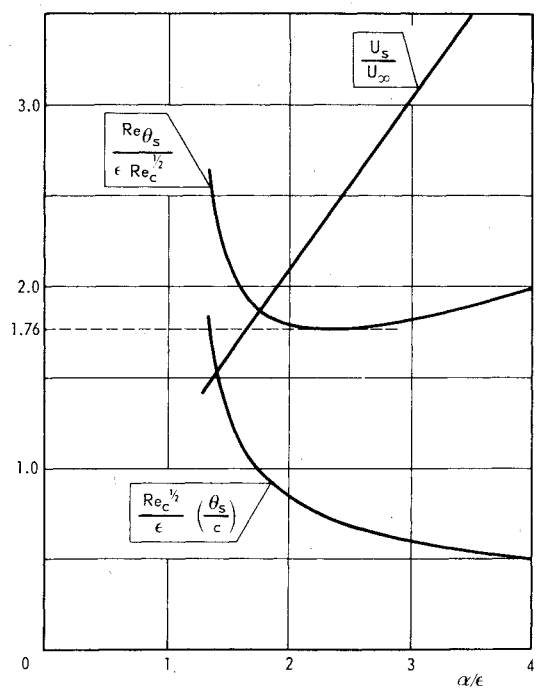

Fig. 2 Some calculated quantities at the laminar separation point.

approximately

$$\frac{U}{U_\infty}=\frac{(\alpha/\epsilon)+(\psi/2\epsilon)}{\{1+(\psi/2\epsilon)^2\}^{1/2}} \tag{2}$$

where α is the angle of attack (rad), and ψ the angle in conformal transformed plane (rad); $\psi=0$ at the leading edge. The angle ψ is related to the distance along the airfoil contour by

$$\mathrm{d}(s/c)=2\epsilon^2\{1+(\psi/2\epsilon)^2\}^{1/2}\mathrm{d}(\psi/2\epsilon) \tag{3}$$

In the derivation of the preceding equations it has been assumed that $\epsilon\ll 1$, $\alpha\ll 1$, and $\psi\ll 1$. Some typical velocity distributions have been plotted in Fig. 1.

Interest is focused here on the laminar boundary-layer properties at separation. Employing Thwaites' calculation method[13] the boundary-layer momentum thickness may be obtained from

$$Re_c\left(\frac{\theta}{c}\right)^2=\frac{0.45}{(U/U_\infty)^6}\int_{s_0/c}^{s/c}\left(\frac{U}{U_\infty}\right)^5\mathrm{d}\frac{s}{c}$$

$$=0.9\epsilon^2\frac{\{1+(\psi/2\epsilon)^2\}^3}{\{(\alpha/\epsilon)+(\psi/2\epsilon)\}^6}\int_{-(\alpha/\epsilon)}^{(\psi/2\epsilon)}\frac{\{(\alpha/\epsilon)+(\psi/2\epsilon)\}^5}{\{1+(\psi/2\epsilon)^2\}^2}\mathrm{d}\frac{\psi}{2\epsilon} \tag{4}$$

The integral in Eq. (4) can be evaluated analytically. The resultant closed-form expression is rather complicated, however, and therefore it will be written here simply

$$\frac{Re_c^{1/2}}{\epsilon}\left(\frac{\theta}{c}\right)=f\left(\frac{\alpha}{\epsilon},\frac{\psi}{2\epsilon}\right) \tag{5}$$

The pressure gradient parameter used in Thwaites' method is

$$\lambda=\frac{\theta^2}{\nu}\frac{\mathrm{d}U}{\mathrm{d}s}=\frac{Re_c}{2\epsilon^2}\left(\frac{\theta}{c}\right)^2\frac{1-(\alpha/\epsilon)(\psi/2\epsilon)}{\{1+(\psi/2\epsilon)^2\}^2} \tag{6}$$

Laminar boundary-layer separation is assumed to take place when $\lambda=\lambda_s=-0.09$. The computed separation positions are indicated in Fig. 1. For $\alpha/\epsilon=1$ no separation was found to occur in the leading-edge region.

The calculated velocity at the separation position, U_s/U_∞, and the laminar boundary-layer momentum thickness, $(Re_c^{1/2}/\epsilon)(\theta_s/c)$, are plotted in Fig. 2 as a function of α/ϵ. The figure also gives the variation of the momentum thickness Reynolds number at separation,

$$Re_{\theta_s}/(\epsilon Re_c^{1/2})=(U_s/U_\infty)(Re_c^{1/2}/\epsilon)(\theta_s/c)$$

As mentioned in the Introduction, the occurrence of bubble burst depends strongly on the momentum thickness Reynolds number at separation.

Another important parameter is the pressure gradient over the bubble, $\Lambda=(\theta_s^2/\nu)(\Delta U/\Delta s)$. At the separation point $\lambda_s=(\theta_s^2/\nu)(\mathrm{d}U/\mathrm{d}s)_s=-0.09$. Consequently one may write

$$\Lambda=-0.09\frac{\Delta U/\Delta s}{(\mathrm{d}U/\mathrm{d}s)_s} \tag{7}$$

This means that the pressure gradient parameter Λ will differ significantly from -0.09 only when the velocity variation over the bubble is distinctly nonlinear. For the moment we will assume that $\Lambda=-0.09$. According to Gaster[4] bubble burst will then occur when $Re_{\theta_s}<125$, i.e., the Owen-Klanfer criterion[2] holds.

Returning now to Fig. 2, it is seen that for a given airfoil ($\epsilon=$ const) and airfoil Reynolds number Re_c, the boundary-layer momentum thickness Reynolds number at separation Re_{θ_s} decreases first with increasing angle of attack and then increases. Bubble burst consequently becomes increasingly unlikely beyond a certain angle of attack. The same conclusion was reached earlier by Ridder[14] and has been confirmed by practical calculations of the flow around airfoils (e.g., Ref. 15). It may further be inferred from Fig. 2 that

$$Re_{\theta_s}/\epsilon Re_c^{1/2}>1.76 \tag{8}$$

It follows that $Re_{\theta_s}>125$ if $\epsilon Re_c^{1/2}>71$. This means that no bubble bursts should be expected to occur for $\epsilon Re_c^{1/2}>71$.

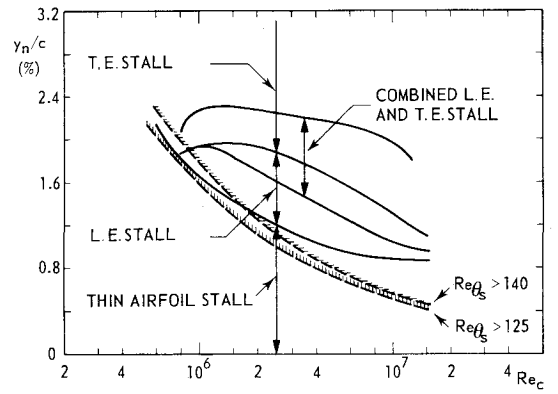

Fig. 3 Gault's graph for types of airfoil stall[1] and calculated lower-bounds for the laminar boundary-layer Reynolds number at separation.

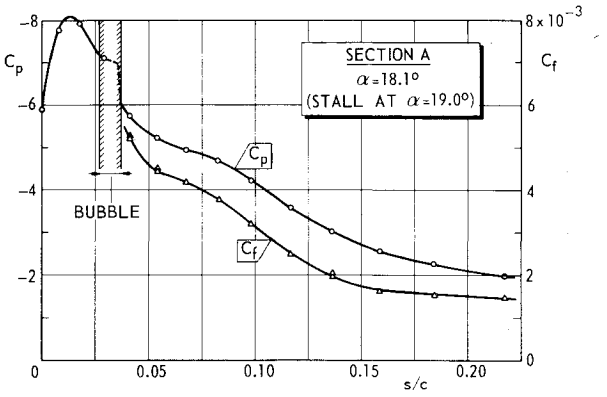

Fig. 4 Experimental wall shear stress and wall pressure data in the leading-edge region of airfoil section A; $Re_c=3\times10^6$.

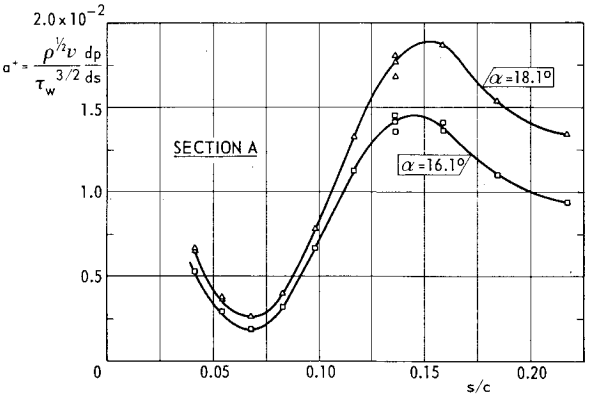

Fig. 5 Separation parameter a^+, derived from measured wall shear stress and pressure gradient, on airfoil section A; $Re_c=3\times10^6$.

Many years ago Gault[1] analyzed a large number of airfoil stalls. His analysis resulted in a graph, which is reproduced in Fig. 3. The graph maps regions for each type of stall as a function of the airfoil Reynolds number Re_c and a characteristic airfoil nose parameter y_n/c, where y_n is the upper surface coordinate at $x/c=1.25\%$. The relation between this parameter and the thickness parameter ϵ may be obtained from Eq. (1); $y_n/c=0.222\epsilon$. So we may also write $Re_{\theta_s}>125$ if $(y_n/c)Re_c^{1/2}>15.8$. This relation is plotted in Fig. 3. No bubble bursts should be expected above the line drawn. It appears that the indicated region for leading-edge stalls is situated at that side of the line. This result suggests that it is unlikely that bubble bursts play a role in leading-edge stalls.

Up to now it has been assumed $\Lambda=-0.09$ and therefore $Re_{\theta_s}<125$ for bubble burst. It follows from Eq. (7) that the actual value of Λ is proportional to the ratio of the mean velocity gradient over the bubble, $\Delta U/\Delta s$, to the gradient at separation, $(dU/ds)_s$. Viewing Fig. 1 it is evident that the ratio generally will be less than one. However, the inflection point of the velocity variation curves is situated downstream of the separation point, so that ratios larger than one are possible. Numerical evaluation gives that, for the velocity variations shown, the ratio will never much exceed 1.1. This yields $\Lambda\approx-0.10$. According to Gaster[4] the corresponding Reynolds number for bubble burst is then $Re_{\theta_s}=140$ at most. The curve above which $Re_{\theta_s}>140$ also is plotted in Fig. 3. This curve extends into the region of leading-edge stalls at low Reynolds numbers. Thus leading-edge stalls by bubble burst may be possible in some cases, but the present analysis suggests these cases to be exceptions and to be restricted to low Reynolds number range leading-edge stalls.

The results of the preceding theoretical analysis may be generalized so far as the basic assumptions can be generalized: the assumption that the velocity distribution in the leading-edge region of symmetrical Joukowski airfoils is typical for general airfoils, and the assumption that Gault's graph is generally valid. Though both generalizations may be questioned, it seems reasonable to conclude that the role of bubble burst in airfoil leading-edge stalls may be rather restricted, especially at higher Reynolds numbers.

Wall Shear-Stress Measurements in the Leading-Edge Region

The wall shear stress variation in the turbulent boundary-layer downstream of the laminar separation bubble has been established on two airfoils. The measurements were carried out in a low-speed wind tunnel using two-dimensional pressure-plotting models. The wall shear-stress data were obtained with the razor-blade technique as introduced by East.[16] This technique is based on the assumption that the law of the wall holds in the wall region of the turbulent boundary layer. The height of the razor blade cutting edge above the wall was 0.125 mm. As the boundary-layer is very thin in the leading-edge region, the razor blade may not have been in the wall region of the boundary layer at all measuring stations. Therefore, the accuracy of the wall shear-stress data may be questioned, particularly for the upstream stations. The accuracy was regarded sufficient, however, for the present aim—to determine how close the boundary layer is to separation.

Figure 4 shows some experimental results obtained with airfoil section A (NLR airfoil 7703) at an angle of attack $\alpha=18.1$ deg. The airfoil exhibits a leading-edge stall, i.e., a sudden loss of lift, at $\alpha=19.0$ deg. The figure gives the wall static pressure distribution in the leading-edge region, the position and extent of the laminar separation bubble as observed with the oil flow technique, and the wall shear-stress development downstream of the bubble. No indication of turbulent boundary-layer separation is obtained from this plot. The wall shear stress coefficient $C_f=\tau_W/\frac{1}{2}\rho U^2$ is, however, a poor parameter for indicating proximity of separation. An acceptable parameter should depend only on wall quantities, since the flow starts to separate there. Wall quantities are, besides properties of the fluid, the wall shear stress itself and the wall pressure gradient. Dimensional analysis then leads to a separation parameter such as

$$a^+=\frac{\rho^{1/2}\nu}{\tau_W^{3/2}}\frac{dp}{ds} \tag{9}$$

The parameter represents the ratio of the pressure forces to the shear forces in wall quantities. The same parameter is generally employed in proposed extensions of the law of the wall for flows with large pressure gradients, including nearly separated flows (e.g., Ref. 17). A large value of a^+ means that the boundary layer is close to separation.

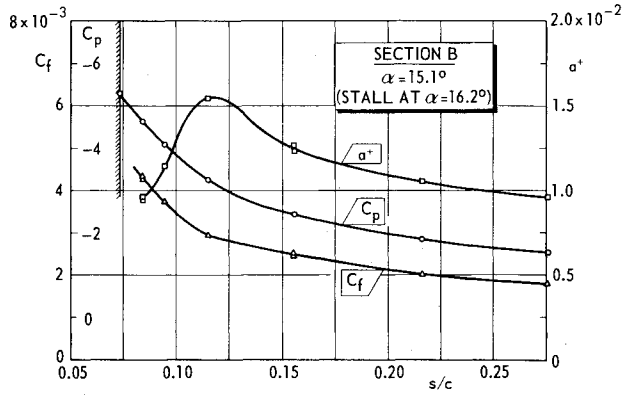

Fig. 6 Wall shear stress and wall pressure data, as well as the separation parameter a^+, on airfoil section B; $Re_c = 2.5 \times 10^6$.

The data from Fig. 4 have been replotted in Fig. 5, now using the separation parameter a^+. The value of a^+ is seen to decrease first, then to increase, to reach a maximum, and to decrease again. It is now evident that the boundary layer may be close to separation at the position of maximum a^+, i.e., at $s/c \approx 0.15$. The graph includes data obtained at a smaller angle of attack, $\alpha = 16.1$ deg. It appears that a^+ increases with increasing angle of attack. At $\alpha = 18.1$ deg the maximum value is close to $a^+ = 2 \times 10^{-2}$. Analyses of flow near the wall, which employ this parameter (e.g., Ref. 18), show that this is already a rather large value for a^+. The shear forces in the wall region are small then. Even in the viscous sublayer they do not dominate over the pressure forces anymore; to cancel the pressure forces at $a^+ = 2 \times 10^{-2}$ the shear stress must nearly double between the wall and the viscous sublayer edge. A complicating factor is that when a^+ is nonnegligible, the wall shear-stress measurement technique employed here is also in error, as it is based on the validity of the law of the wall, i.e., on the assumption that $a^+ = 0$. It can be shown, that for $a^+ > 0$ the measured wall shear stress will be large, so that the correct values for a^+ will be larger than the values given here. Summarizing, it may be concluded that the measurements suggest that the leading-edge stall of this airfoil is due to turbulent boundary-layer separation at $s/c \approx 0.15$. It should be noted that the turbulent boundary-layer separation point, though situated in the leading-edge region, is not close behind the laminar separation bubble.

Figure 6 shows the measurement results at $\alpha = 15.1$ deg for airfoil section B (NLR airfoil 7301), which exhibits a leading-edge stall at $\alpha = 16.2$ deg. Again no indication of separation is obtained from the measured wall shear-stress variation. The separation parameter a^+, however, is seen to increase significantly downstream of the bubble and subsequently to reach a maximum. It may be concluded that for this airfoil turbulent boundary-layer separation at $s/c \approx 0.12$ is the probable cause of the stall.

Conclusions

1) An approximate theoretical analysis of the flow near airfoil leading edges suggests that bursting of the laminar separation bubble is not the cause of most leading-edge stalls, especially not leading-edge stalls at higher Reynolds numbers.

2) Wall shear-stress measurements, which were carried out on two airfoils, indicate that turbulent boundary-layer separation somewhere in the leading-edge region is the probable cause of the leading-edge stall of these airfoils.

3) Though the direct role of the bubble in leading-edge stalls may be restricted, indirectly its role can be significant as it determines the initial conditions of the turbulent boundary layer downstream.

References

[1] Gault, D. E., "A Correlation of Low-Speed Airfoil Section Stalling Characteristics with Reynolds Number and Airfoil Geometry," NACA TN 3963, 1957.

[2] Owen, P. R. and Klanfer, L., "On the Laminar Boundary Layer Separation from the Leading Edge of a Thin Airfoil," Aeronautical Research Council, Britain, Current Paper 220, 1955.

[3] Crabtree, L. F., "Effects of Leading Edge Separation on Thin Wings in Two-Dimensional Incompressible Flow," *Journal of the Aeronautical Sciences,* Vol. 24, Aug. 1957, pp. 597-604.

[4] Gaster, M., "The Structure and Behaviour of Laminar Separation Bubbles," AGARD *Conference Proceedings 4,* 1966, pp. 819-854.

[5] Horton, H. P., "A Semi-Empirical Theory for the Growth and Bursting of Laminar Separation Bubbles," Aeronautical Research Council, Britain, Current Paper 1073, 1967.

[6] Vincent de Paul, M., "Prévision du Décrochage d'un Profil d'Aile en Ecoulement Incompressible," *AGARD Conference Proceedings 102,* 1972.

[7] Ingen, J. L. van, "On the Calculation of Laminar Separation Bubbles in Two-Dimensional Incompressible Flow," *AGARD Conference Proceedings 168,* 1975.

[8] Roberts, W. B., "The Effect of Reynolds Number and Laminar Separation on Axial Cascade Performance," *ASME Journal of Engineering for Power,* April 1975, pp. 261-274.

[9] Wallis, R. A., "Experiments with Air Jets to Control the Nose Stall on a 3 ft Chord NACA 64A006 Aerofoil," Aeronautical Research Laboratories, Australia, Aero Note 139, 1954.

[10] Hurley, D. G., "The Downstream Effect of a Local Thickening of the Laminar Boundary Layer," Aeronautical Research Laboratories, Australia, Aero Note 146, 1955.

[11] Evans, T. E. and Mort, K. W., "Analysis of Computed Flow Parameters for a Set of Sudden Stalls in Low-Speed Two-Dimensional Flow," NASA TN D-85, 1959.

[12] Schlichting, H. and Truckenbrodt, E., *Aerodynamik des Flugzeuges,* 1st ed., Vol. 1, Springer Verlag, Berlin, 1959, p. 386.

[13] Thwaites, B., "Approximate Calculation of the Laminar Boundary Layer," *Aeronautical Quarterly,* Vol. 1, Nov. 1949, pp. 245-280.

[14] Ridder, S. O., "Experimental Studies of the Leading Edge Suction Force, Including the Maximum Attainable Suction Force versus Reynolds Number and the Induced Distributions on Various Wing Planforms and Air Intakes," *ICAS Conference Proceedings,* Vol. 1, 1974, pp. 302-396.

[15] Oskam, B., "A Calculation Method of the Viscous Flow around Multi-component Airfoils," National Aerospace Laboratory, Netherlands, NLR TR 79097, 1980.

[16] East, L. F., "Measurement of Skin Friction at Low Subsonic Speeds by the Razor Blade Technique," Royal Aircraft Est., Britain, RAE TR 66277, 1966.

[17] Townsend, A. A., "Equilibrium Layers and Wall Turbulence," *Journal of Fluid Mechanics,* Vol. 11, Aug. 1961, pp. 97-119.

[18] Berg, B. van den, "A Three-Dimensional Law of the Wall for Turbulent Shear Flows," *Journal of Fluid Mechanics,* Vol. 70, July 1975, pp. 149-160.